# A resolution of the missing charge problem in nuclear Coulomb sum*

K. Miyazaki

**Abstract**

At high momentum transfer $|\mathbf{q}| > 1\,\mathrm{GeV}$, the longitudinal response in quasi-elastic electron scattering off nuclei is well reproduced by the free Fermi gas model. This suggests the suppression of the Z-graph contributions in elementary electron-nucleon scattering in nuclear medium. Therefore we develop the relativistic model in which those contributions are partially suppressed. The suppression redefines the relativistic effective mass and introduces the effective charge of a nuclear nucleon scattering the electrons. These quantities reproduce both the position and height of the quasi-elastic peak. Consequently, the missing charge problem is also naturally explained.

## 1 Introduction

Recently there are renewed interests [1-3] on the longitudinal response function in quasi-elastic electron scattering from the viewpoint of the relativistic nuclear matter model. They are inspired by the fact that the response for $^{56}$Fe at $|\mathbf{q}| = 1140\,\mathrm{MeV}$ [4] is well reproduced by the free Fermi gas model rather than the relativistic Hartree model [5]. It suggests the suppression of the relativistic medium effect at high momentum transfer. Frank [1] pointed out that the suppression is due to momentum dependence of the scalar and vector self-energies of a nucleon in nuclear medium. He phenomenologically introduced a step function to describe the momentum-dependent self-energies. Chen and Ma [2] and Kim, Horowitz and Frank [3] refined Frank's work by using more realistic momentum dependencies. In Ref. [2] the result of the relativistic Bruekner-Hartree-Fock calculation was employed, while in Ref. [3] phenomenological nucleon-nucleus optical potentials were utilized. These works can reproduce the longitudinal response for $^{56}$Fe at $|\mathbf{q}| = 550\,\mathrm{MeV}$ and $1140\,\mathrm{MeV}$ in the range of the energy transfer $\omega$ below the quasi-elastic peak. However the position and height of the peak, which are essential ingredients in the quasi-elastic picture, cannot be reproduced. We are not contented unless both the quantities are well reproduced simultaneously.

The quasi-elastic peak positions of the longitudinal responses at $|\mathbf{q}| = 550\,\mathrm{MeV}$ and $1140\,\mathrm{MeV}$ suggest that the effective mass of a target nucleon scattering the electrons

*This paper is the revised version of CDS ext-2002-049. Some texts and mistypes have been corrected.

becomes larger than that obtained from the relativistic mean-field theory [6]. Now we remember that the successes of the relativistic models are essentially due to the virtual $N\bar{N}$ pair effect [7,8]. Therefore such an enhancement of the effective mass may be owing to the suppression of the virtual $N\bar{N}$ pairs or the Z-graph contributions in elementary electron-nucleon ($eN$) scattering. However the criticisms to the relativistic models [9-11] are also concentrated on the $N\bar{N}$ pair contribution because it corresponds to $(qqq)\,(\bar{q}\bar{q}\bar{q})$ in a quark picture of the nucleons and such a simultaneous three $\bar{q}$ creation should be suppressed by taking into account the composite nature of the nucleons. On the other hand, it was shown [12,13] that the nucleon Z-graph at nearly zero transferred momentum is equivalent to the single quark Z-graph but not to three quark Z-graph. Consequently, it is believed that the relativistic models are valid only at low momentum transfers while the nucleon Z-graph contributions should be suppressed at high momentum transfers. In the next section we develop a phenomenological model to suppress the effects of the Z-graph on the quasi-elastic electron scattering. In section 3 the numerical results of the longitudinal responses for $^{56}$Fe at medium and high momentum transfer are given. Finally we summarize in section 4.

# 2 Suppression of the Z-graph

In order to investigate the effects of the Z-graph contributions in quasi-elastic electron scattering, we first note that the positive-energy Dirac spinor in nuclear medium $u_*(\mathbf{p},s)$ with mass $M^*$ is expanded by the positive and negative-energy Dirac spinors in the free space, $u(\mathbf{p},s)$ and $w(\mathbf{p},s)$ with mass $M$ [14]:

$$u_*(\mathbf{p},s) = \left(\frac{E_p^*+M^*}{2E_p^*}\right)^{1/2}\begin{pmatrix}1\\ \boldsymbol{\sigma}\cdot\mathbf{p}/\left(E_p^*+M^*\right)\end{pmatrix}\chi_s, \tag{1}$$

$$= \cos\theta_p\, u(\mathbf{p},s) + \sin\theta_p \sum_{s'}\langle s'|\,\boldsymbol{\sigma}\cdot\mathbf{p}\,|s\rangle\, w(\mathbf{p},s'), \tag{2}$$

where

$$u(\mathbf{p},s) = \left(\frac{E_p+M}{2E_p}\right)^{1/2}\begin{pmatrix}1\\ \boldsymbol{\sigma}\cdot\mathbf{p}/\left(E_p+M\right)\end{pmatrix}\chi_s, \tag{3}$$

$$w(\mathbf{p},s) = \left(\frac{E_p+M}{2E_p}\right)^{1/2}\begin{pmatrix}-\boldsymbol{\sigma}\cdot\mathbf{p}/\left(E_p+M\right)\\ 1\end{pmatrix}\chi_s, \tag{4}$$

$E_p^* = \left(|\mathbf{p}|^2+(M^*)^2\right)^{1/2}$, $E_p = \left(|\mathbf{p}|^2+M^2\right)^{1/2}$ and $\chi_s$ is the Pauli spinor. The mixing angle $\theta_p$ between the positive and negative-energy states is given by [14]

$$\tan(2\,\theta_p) = \frac{|\mathbf{p}|\,(M-M^*)}{|\mathbf{p}|^2+MM^*}. \tag{5}$$

Here we note that $\theta_p \ll 1$ in Eq. (2) or

$$\tan(2\,\theta_p) \approx \sin(2\,\theta_p) \approx 2\,\theta_p = \frac{|\mathbf{p}|\,(M - M^*)}{|\mathbf{p}|^2 + M\;M^*}, \tag{6}$$

as shown in Fig. 1. Thus Eq. (2) is approximately rewritten by

$$u_*(\mathbf{p}, s) \approx u(\mathbf{p}, s) + \theta_p \sum_{s'} \langle s' |\, \boldsymbol{\sigma} \cdot \mathbf{p}\, | s \rangle\, w(\mathbf{p}, s')\,. \tag{7}$$

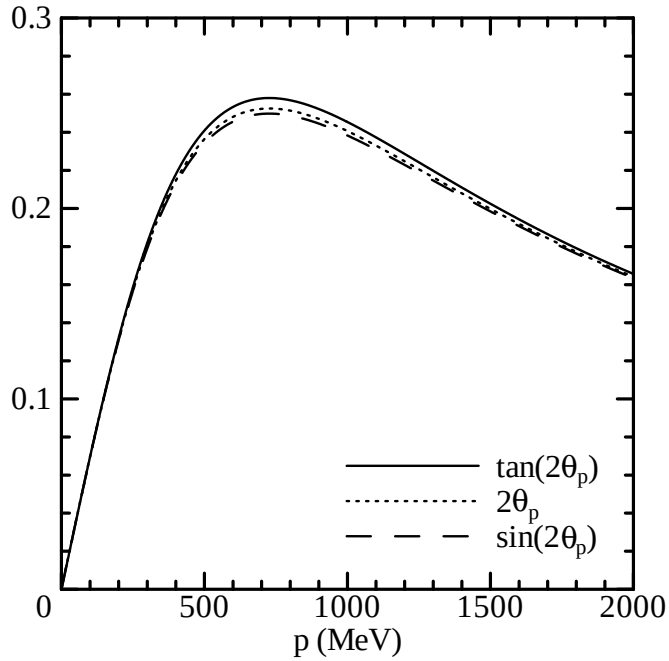


Figure 1: The momentum dependence of the mixing angle between the positive and negative energy states defined by Eq. (5). The solid, dotted and long-dashed curves denote $\tan(2\theta_p)$, $2\theta_p$ and $\sin(2\theta_p)$ respectively. We asume the value of the scalar potential $S = -375\,\mathrm{MeV}$.

Then we consider the current matrix

$$\langle\, \bar{u}_*(\mathbf{p}', s') |\, J^\mu \,|\, u_*(\mathbf{p}, s)\,\rangle \tag{8}$$

Using Eq. (2) or (7), this is composed of the four contributions as

$$\langle\, \bar{u}(\mathbf{p}', s') |\, J^\mu \,|\, u(\mathbf{p}, s)\,\rangle \;:\; (++)\ \text{coupling}, \tag{9}$$

$$\langle\, \bar{u}(\mathbf{p}', s') |\, J^\mu \,|\, w(\mathbf{p}, s)\,\rangle \;:\; (+-)\ \text{coupling}, \tag{10}$$

$$\langle\, \bar{w}(\mathbf{p}', s') |\, J^\mu \,|\, u(\mathbf{p}, s)\,\rangle \;:\; (-+)\ \text{coupling}, \tag{11}$$

$$\langle\, \bar{w}(\mathbf{p}', s') |\, J^\mu \,|\, w(\mathbf{p}, s)\,\rangle \;:\; (--)\ \text{coupling}. \tag{12}$$

Difference between the nuclear matter and the Fermi gas is due to $(+-)$ (or $(-+)$)

coupling. Because the mixing of $w(\mathbf{p},s)$ in $u_*(\mathbf{p},s)$ is essentially due to the scalar potential $S$, the $(+-)$ coupling means the following Z-graph contribution in elementary $eN$ scattering:

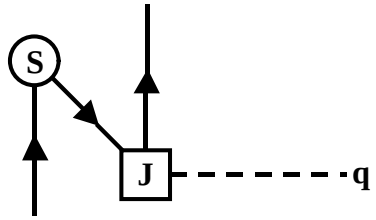


If the transferred momentum $|\mathbf{q}|$ becomes large, the electron sees the inside of nucleon. In this case, the electron (or virtual photon) interacts with the quark in nucleon but not the nucleon itself. Thus the above nucleon Z-graph contributions should be partially suppressed. Unfortunately, the theoretical derivation of such suppression is difficult. In the present work we will partially suppress the $(+-)$ and $(-+)$ coupling in a phenomenological way.

For this purpose we artificially multiply Eq. (10) by the suppression factor $\lambda(|\mathbf{q}|)$:

$$\lambda(|\mathbf{q}|)\,\langle\,\bar{u}\,(\mathbf{p}',s')|\,J^{\mu}\,|\,w\,(\mathbf{p},s)\,\rangle\,. \tag{13}$$

The factor $\lambda(|\mathbf{q}|)$ shall satisfy the condition

$$\lambda(|\mathbf{q}|)=\begin{cases}=1\ :\ |\mathbf{q}|=0,\\ \ll 1\ :\ |\mathbf{q}|>M.\end{cases} \tag{14}$$

So as to replace Eq. (10) by Eq. (13), we modify the current matrix (8) as

$$\langle\,\bar{u}_*\,(\mathbf{p}',s')|\,\bar{\Lambda}_{\lambda}\,(\mathbf{p}')\,J^{\mu}\Lambda_{\lambda}\,(\mathbf{p})\,|\,u_*\,(\mathbf{p},s)\rangle\,, \tag{15}$$

where

$$\Lambda_{\lambda}\,(\mathbf{p})=\Lambda^{+}\,(\mathbf{p})+\lambda\,\Lambda^{-}\,(\mathbf{p})\,, \tag{16}$$

with the projection operators to the positive $(\Lambda^{+})$ and negative $(\Lambda^{-})$ energy states:

$$\Lambda^{+}\,(\mathbf{p})=\sum_{s}u\,(\mathbf{p},s)\,u^{\dagger}\,(\mathbf{p},s)=\frac{\not{p}+M}{2E_p}\,\gamma^{0}, \tag{17}$$

$$\Lambda^{-}\,(\mathbf{p})=\sum_{s}w\,(\mathbf{p},s)\,w^{\dagger}\,(\mathbf{p},s)=\gamma^{0}\,\frac{\not{p}-M}{2E_p}. \tag{18}$$

However $\Lambda_{\lambda}\,(\mathbf{p})$ is not a projection operator and so Eq. (15) does not satisfy the current conservation

$$\langle\,\bar{u}_*\,(\mathbf{p}',s')|\,\bar{\Lambda}_{\lambda}\,(\mathbf{p}')\,q_{\mu}J^{\mu}\,\Lambda_{\lambda}\,(\mathbf{p})\,|\,u_*\,(\mathbf{p},s)\rangle=\lambda\,(1-\lambda)\,(M-M^{*})\,\left(\cos\theta'_p-\cos\theta_p\right)\neq 0, \tag{19}$$

except that $\lambda(|\mathbf{q}|)$ is a step function as $\lambda(|\mathbf{q}|) = \theta(|\mathbf{q}| - q_c)$ with cut-off momentum $q_c$. Although the strict theoretical derivation of the suppression factor $\lambda(|\mathbf{q}|)$ is beyond the present work as mentioned above, it should be related to the nucleon structure function and thus is not a step function. At present it is reasonable to assume the Sachs form factor $G_E(|\mathbf{q}|)$ as $\lambda(|\mathbf{q}|)$, which satisfies the condition (14):

$$\lambda(|\mathbf{q}|) = G_E(|\mathbf{q}|) = \left(1 + |\mathbf{q}|^2/c\right)^{-2} \quad \text{with} \quad c = 0.71\,\text{GeV}^{-2}. \tag{20}$$

Because within the picture of point-like nucleons $G_E(|\mathbf{q}|)$ is regarded as the probability for electrons with momentum $\mathbf{q}$ to see a whole nucleon as a point particle, the Z-graph of a point-like nucleon should be weighted with the probability. Although the current $J^\mu$ in Eq. (13) already contains the form factors, the weighting factor of Eq. (20) does not cause double counting since the Z-graph is the second-order contribution as seen in the above picture.

Now we have to recover the current conservation. For this purpose, it is noted that the Dirac spinor $u_*(\mathbf{p}, s)$ with mass $M^*$ can be also expanded by the Dirac spinors $u_\lambda(\mathbf{p}, s)$ and $w_\lambda(\mathbf{p}, s)$ with any mass $M_\lambda$ similar to Eq. (7):

$$u_*(\mathbf{p}, s) \approx u_\lambda(\mathbf{p}, s) + \theta_p^\lambda \sum_{s'} \langle s' | \boldsymbol{\sigma} \cdot \mathbf{p} | s \rangle w_\lambda(\mathbf{p}, s'). \tag{21}$$

Then we demand that $\Lambda_\lambda(\mathbf{p}) u_*(\mathbf{p}, s)$ in Eq. (15) can be replaced by $N_\lambda u_\lambda(\mathbf{p}, s)$ with appropriate value of mass $M_\lambda$ and normalization factor $N_\lambda$. As a result, the current matrix becomes

$$N_\lambda^2 \langle \bar{u}_\lambda(\mathbf{p}', s') | J^\mu(q) | u_\lambda(\mathbf{p}, s) \rangle, \tag{22}$$

in place of Eq. (8). An appropriate value of $M_\lambda$ can be defined as follows. We have supposed that Eq. (22) gives the reduced $(+-)$ coupling of Eq. (13). Therefore it is expected that the new Dirac spinor $u_\lambda(\mathbf{p}, s)$ is expressed by

$$u_\lambda(\mathbf{p}, s) \approx u(\mathbf{p}, s) + \lambda \theta_p \sum_{s'} \langle s' | \boldsymbol{\sigma} \cdot \mathbf{p} | s \rangle w(\mathbf{p}, s'). \tag{23}$$

in place of Eq. (7). Defining a new mixing angle $\phi_p$ between the positive and negative-energy states as

$$\phi_p \equiv \lambda \theta_p = \frac{1}{2} \frac{|\mathbf{p}| (M - M_\lambda)}{|\mathbf{p}|^2 + M M_\lambda}, \tag{24}$$

the corresponding effective mass $M_\lambda$ is given by

$$M_\lambda = \frac{M\left(|\mathbf{p}|^2 + M M^*\right) - \lambda (M - M^*) |\mathbf{p}|^2}{|\mathbf{p}|^2 + M M^* + \lambda M (M - M^*)}. \tag{25}$$

This satisfies the conditions

$$M_{\lambda=0} = M, \tag{26}$$

$$M_{\lambda=1} = M^*. \tag{27}$$

Since the momentum dependence of $M_\lambda$ is troublesome, we replace $|\mathbf{p}|^2$ in Eq. (27) by $M\,M^*$ which gives the maximum value of $\theta_p$. This approximation is reasonable because of the weak dependence of $M_\lambda$ on $|\mathbf{p}|$ as shown in Fig. 2. Consequently, the appropriate value of $M_\lambda$ for the current matrix (22) is

$$M_\lambda \approx \frac{2M - \lambda\,(M - M^*)}{2M^* + \lambda\,(M - M^*)} M^*. \tag{28}$$

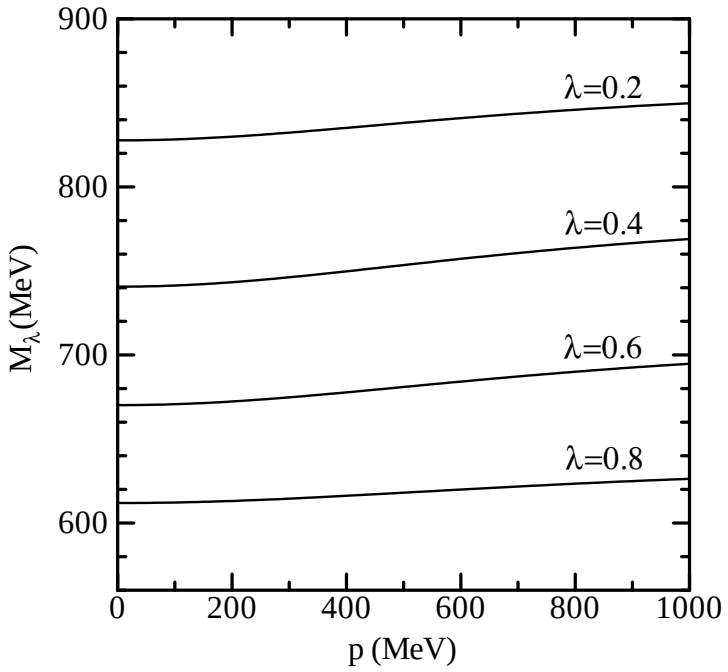


Figure 2: The effective mass $M_\lambda$ defined by Eq. (25) as functions of $|\mathbf{p}|$ for $\lambda = 0.2$, 0.4, 0.6 and 0.8.

Next, the value of the renormalization constant $N_\lambda$ has to be determined. Although $N_\lambda \approx 1$, we cannot set $N_\lambda = 1$ because it determines the height of the quasi-elastic peak through the effective charge $e_\lambda^{eff}$ of a target nucleon. (Note $N_\lambda < 1$.)

$$e_\lambda^{eff} \equiv N_\lambda^2\, e. \tag{29}$$

Here $N_\lambda$ is defined by

$$N_\lambda \equiv \left[ u_\lambda^\dagger\,(\mathbf{p}, s)\,(\,\Lambda_\lambda\,(p)|_{\,p^0 = E_\lambda}\,)\,u_\lambda\,(\mathbf{p}, s) \right]_{\mathbf{p}=\mathbf{0}}. \tag{30}$$

Although $p^0 = E_p$ in the original definition of $\Lambda_\lambda\,(p)$ in Eq. (16), $p^0 = E_\lambda \equiv \left(|\mathbf{p}|^{\,2} + M_\lambda^2\right)^{1/2}$

has been assumed. Furthermore we have taken $\mathbf{p} = \mathbf{0}$ corresponding to the quasi-elastic peak position. Consequently,

$$N_\lambda = \frac{1}{2}\left[(1 + m_\lambda) + \lambda\,(1 - m_\lambda)\right], \tag{31}$$

where $m_\lambda \equiv M_\lambda / M$. Comparing Eqs. (7) and (23), $u_\lambda(\mathbf{p}, s)$ returns to $u_*(\mathbf{p}, s)$ for $\lambda = 1$ while it reduces to $u(\mathbf{p}, s)$ for $\lambda = 0$ and the Z-graph contributions are completely suppressed. For $0 < \lambda < 1$ they are partially suppressed.

Now we have seen that the suppression of the nucleon Z-graph contributions can be accounted by using effective mass $M_\lambda$ and effective charge $e_\lambda^{eff}$ in place of $M^*$ and $e$. This only means that the incident electrons (or virtual photons) see the target nucleus as a collection of the nucleons with mass $M_\lambda$ and charge $e_\lambda^{eff}$. The properties of nuclear matter is determined by $M^*$ but not by $M_\lambda$.

# 3 Results and analyses

Here we show the numerical results of the longitudinal response $R_L$. Our model is not appropriate for the transverse response $R_T$ because we have simply chosen the nucleon charge distribution as the Z-graph suppression factor in Eq. (20). Our calculation of $R_L$ is equivalent to the relativistic mean-field model except for the effective mass $M_\lambda$ and the effective charge $e_\lambda^{eff}$, which depend on transferred momentum $|\mathbf{q}|$. We take the value of the scalar potential as $S = -375\,\mathrm{MeV}$. This value corresponds to $M^*/M \simeq 0.6$ and is reasonable for the relativistic nuclear matter saturation properties [15].

Figures 3 and 4 show $R_L$ for $^{56}$Fe at $|\mathbf{q}| = 550\,\mathrm{MeV}$ and $1140\,\mathrm{MeV}$. The solid, dashed and dotted curves are the results of our model, relativistic mean-field model and the free Fermi gas model respectively. The agreement of our model with the experimental data [4,16] is quite good except that the quasi-elastic peak position shifts to somewhat higher energy transfer at $|\mathbf{q}| = 1140\,\mathrm{MeV}$. The relativistic mean-field model can reproduce neither the position nor the height of the quasi-elastic peak. The free Fermi gas model provides too high quasi-elastic peak at $|\mathbf{q}| = 550\,\mathrm{MeV}$. Our results are also superior to the models of Refs. [2] and [3]. These indicate that the Z-graph contributions in elementary $eN$ scattering are really suppressed.

It is noted that our model has no fitted parameters. Values of the Z-graph suppression factor $\lambda(|\mathbf{q}|)$ given by Eq. (20) are $\lambda = 0.492$ at $|\mathbf{q}| = 550\,\mathrm{MeV}$ and $\lambda = 0.125$ at $|\mathbf{q}| = 1140\,\mathrm{MeV}$. Therefore the Z-graph contributions are rather suppressed even at medium momentum transfer $|\mathbf{q}| = 550\,\mathrm{MeV}$ and are largely suppressed at high momentum transfer $|\mathbf{q}| = 1140\,\mathrm{MeV}$. Figure 5 shows the ratio of the effective mass $M_\lambda$ to the physical mass $M$ as a function of $|\mathbf{q}|$. In the region $|\mathbf{q}| < 1\,\mathrm{GeV}$, $M_\lambda$ rapidly changes with increasing $|\mathbf{q}|$ while the change is slow for $|\mathbf{q}| > 1\,\mathrm{GeV}$. This indicates that the Z-graph contributions are rapidly suppressed with increasing $|\mathbf{q}|$ up to $1\,\mathrm{GeV}$.

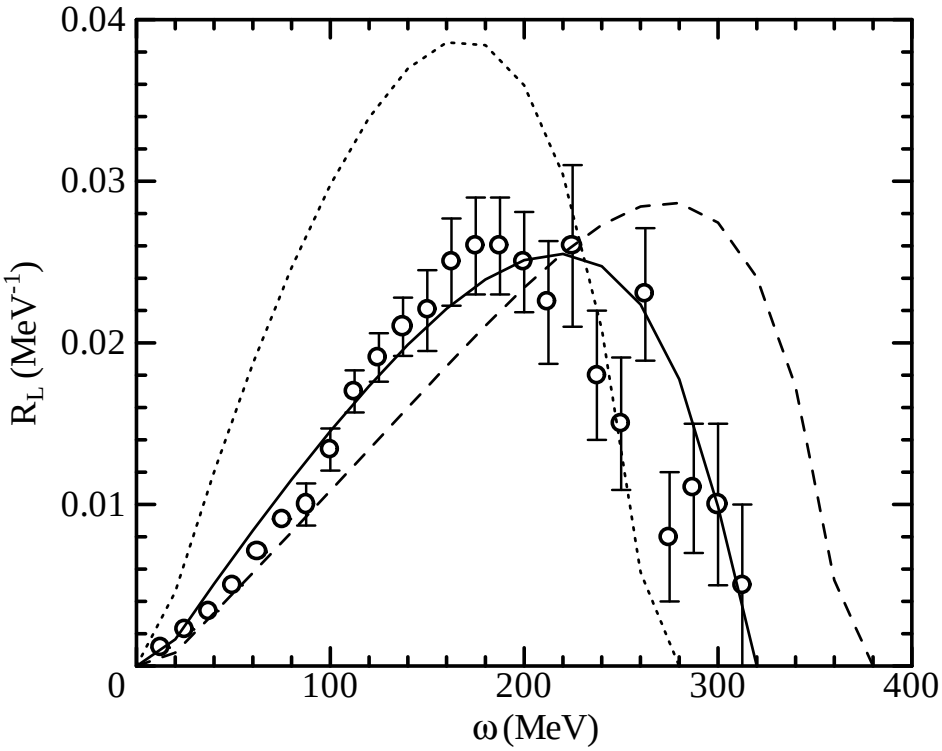


Figure 3: The longitudinal response at $|\mathbf{q}| = 550\,\mathrm{MeV}$ for $^{56}$Fe. The solid, dashed and dotted curves are the results of our model, the relativistic mean-field model and the free Fermi gas model respectively. Experimental data are from Ref. [16].

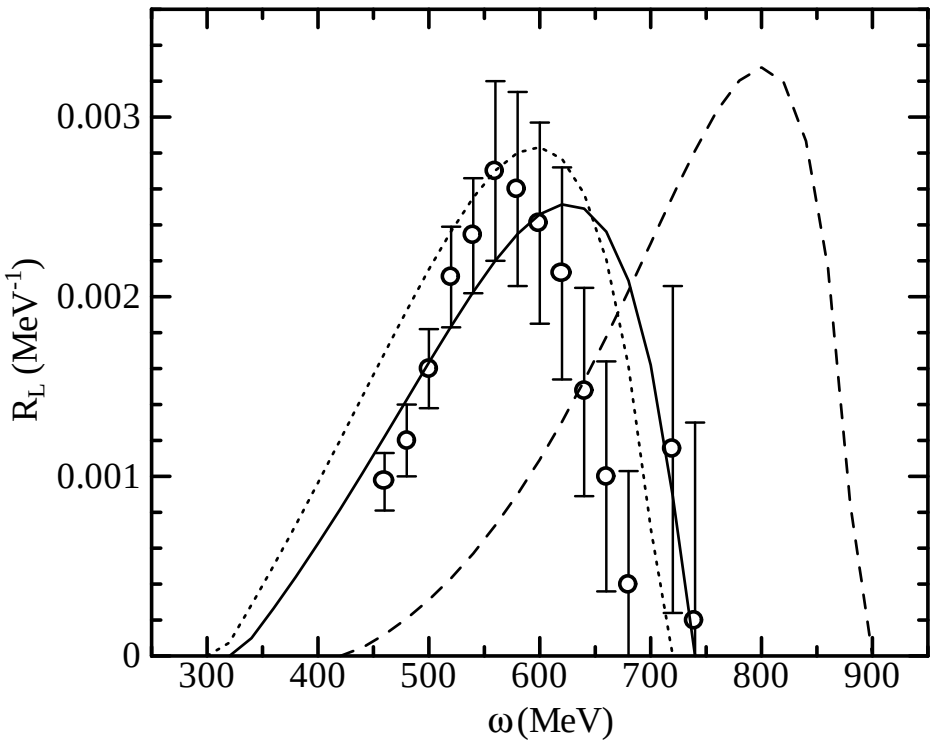


Figure 4: The same as Fig. 3 but for $|\mathbf{q}| = 1140\,\mathrm{MeV}$. Experimental data are from Ref. [4].

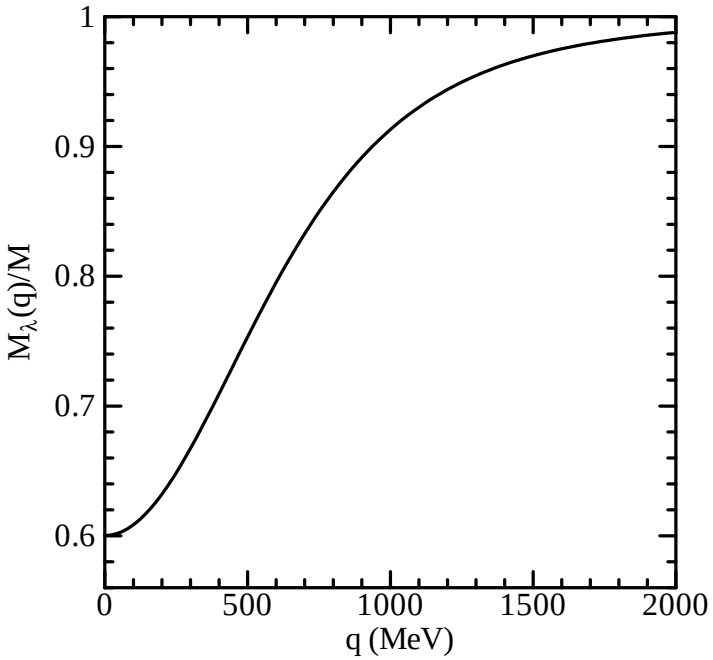


Figure 5: The ratio of the effective mass $M_\lambda$ to the physical mass $M$ as a function of transferred momentum $|\mathbf{q}|$.

The height of the quasi-elastic peak depends on the effective charge $e_\lambda^{eff}$. Figure 6 shows the dependence of $e_\lambda^{eff}$ on $|\mathbf{q}|$. We can see that the effective charge apparently decreases from the physical charge $e$ around $|\mathbf{q}| = 576\,\mathrm{MeV}$. This is the reason of the success of our model at $|\mathbf{q}| = 550\,\mathrm{MeV}$. The effective charge is also concerned with the so-called missing charge problem. Although Jourdan [17] suggested no missing-problem from re-analysis of the world data, Morgenstern and Meziani [18,19] recently criticize it and we here follow their assertion. Then the Coulomb sum [5] is calculated in Fig. 7. Experimental data [16] is well reproduced over the wide range of momentum transfer. Our effective charge has resolved the missing charge problem. Here we want to emphasize that other models [20,21], which are able to reproduce the Coulomb sum, use the larger values of the effective mass $M^*$ than 0.6 taken in our model. However their values are not appropriate for nuclear matter saturation properties and strong spin-orbit potentials. On the contrary we have used $M_\lambda$ in place of $M^*$. This redefined effective mass is derived from $M^*$ through the suppression of Z-graph, and so does not conflict with nuclear matter saturation properties.

Finally, we mention the relation of the present model to the picture of swollen nucleon [21,22] in nuclear medium. Although the effective charge has been defined in Eq. (29), we can incorporate the renormalization factor $N_\lambda$ into the form factor of the nucleons. Then the Sachs form factor becomes

$$G_E^*\left(|\mathbf{q}|\right) = N_\lambda^2\left(|\mathbf{q}|\right) G_E\left(|\mathbf{q}|\right). \tag{32}$$

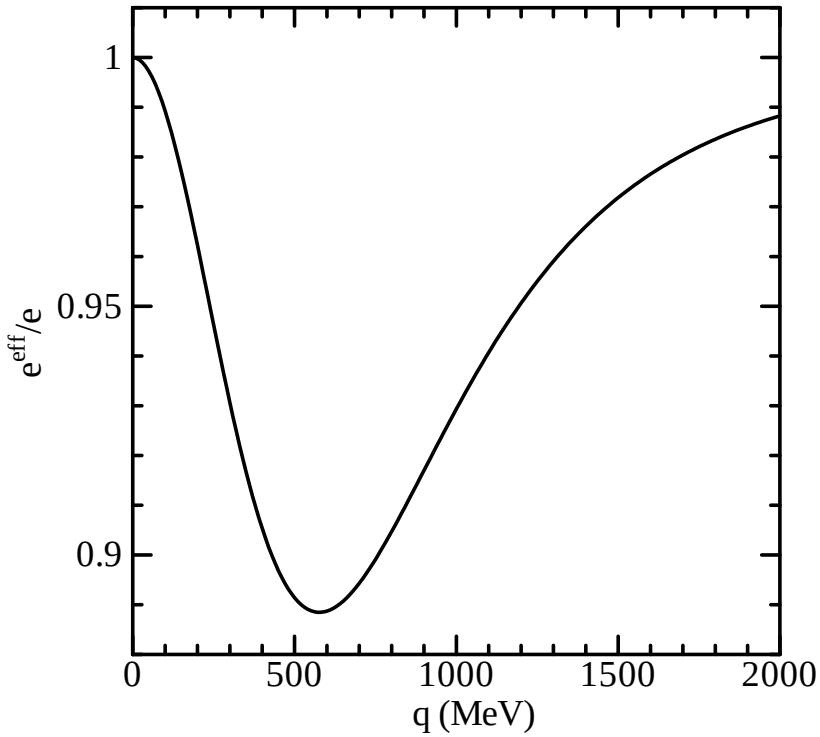


Figure 6: The ratio of the effective charge $e_\lambda^{eff}$ to the physical charge $e$ as a function of transferred momentum $|\mathbf{q}|$.

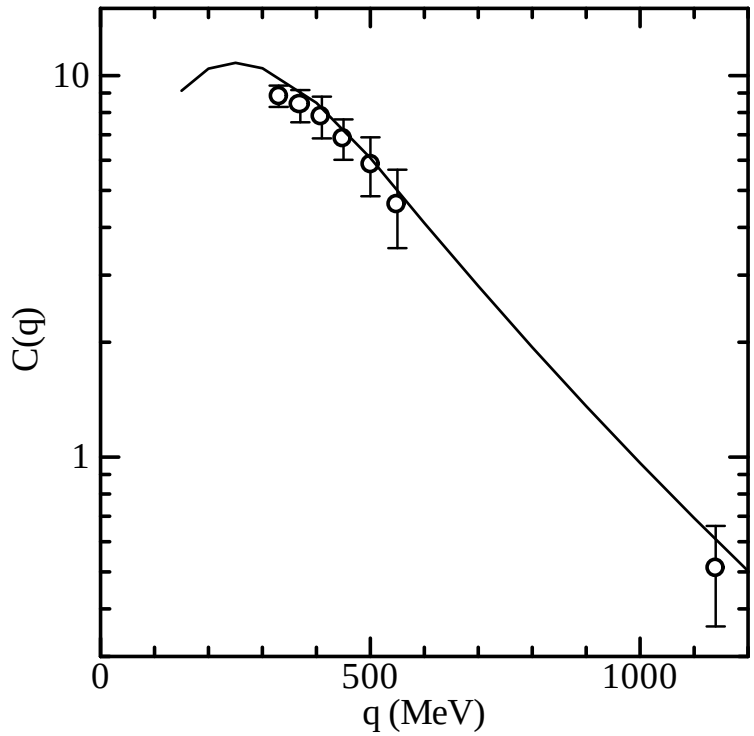


Figure 7: Coulomb sum $C\left(|\mathbf{q}|\right)$ for $^{56}$Fe as a function of transferred momentum $|\mathbf{q}|$. Experimental data are from Ref. [16].

Therefore

$$\left.\frac{dG_E^*}{d\,\mathbf{q}^2}\right|_{\mathbf{q}^2=0} = \left.\frac{dG_E}{d\,\mathbf{q}^2}\right|_{\mathbf{q}^2=0} + 2\left.\frac{dN_\lambda}{d\,\mathbf{q}^2}\right|_{\mathbf{q}^2=0}. \tag{33}$$

Using Eq. (31) we have

$$\left.\frac{dN_\lambda}{d\,\mathbf{q}^2}\right|_{\mathbf{q}^2=0} = \frac{1}{2}\left(1-m^*\right)\left.\frac{d\lambda}{d\,\mathbf{q}^2}\right|_{\mathbf{q}^2=0}. \tag{34}$$

Because $\lambda\left(|\mathbf{q}|\right) = G_E\left(|\mathbf{q}|\right)$ from Eq. (20), the charge radius is

$$\left\langle r_p^2\right\rangle^* \equiv -6\left.\frac{dG_E^*}{d\,\mathbf{q}^2}\right|_{\mathbf{q}^2=0} = \left(2-m^*\right)\left\langle r_p^2\right\rangle. \tag{35}$$

As a result the charge radius of nuclear nucleon becomes larger by about 18% than that of the free nucleon using $m^* = 0.6$. This value is smaller than 30% swelling obtained by other works. This is due to our choice of $\lambda\left(|\mathbf{q}|\right) = G_E\left(|\mathbf{q}|\right)$, which explains the longitudinal responses of quasi-elastic electron scattering well in the region $|\mathbf{q}| > 500\,\mathrm{MeV}$ as shown above. However it might be invalid at small $|\mathbf{q}|$ region where the charge radius is determined. We note that the picture of quasi-elastic scattering becomes invalid at small $|\mathbf{q}|$, and so it is difficult to derive the charge radius of nuclear nucleon.

# 4 Conclusion

We have investigated the effects of the suppression of the nucleon Z-graph contributions in the relativistic model for quasi-elastic electron scattering. They are accounted by introducing the new effective mass $M_\lambda$ and the effective charge $e_\lambda^{eff}$ of nuclear nucleon that the incident electrons see. The longitudinal responses for $^{56}$Fe at medium and high transferred momentum are well reproduced. This indicates that the nucleon Z-graph in elementary $eN$ scattering is really suppressed. Although our model has no fitted parameters, there is an uncertainty in determining the suppression factor $\lambda\left(|\mathbf{q}|\right)$ with which the Z-graph contributions are weighted. We naively assumed the nucleon form factor for it. However this choice has no theoretical foundations. It is a challenging subject to study the mechanism of the Z-graph suppression from more fundamental theoretical viewpoint.

# References


[1] M.R. Frank, Phys. Rev. **C49**, 555 (1994).

[2] Baoqui Chen and Zhongyu Ma, Phys. Lett. **B339**, 297 (1994).

[3] Hungchong Kim, C.J. Horowitz and M.R. Frank, Phys. Rev. **C51**, 792 (1995).

[4] J.P. Chen et al., Phys. Rev. Lett. **66**, 1283 (1991).

[5] K. Wehrberger, Phys. Rep. **225**, 273 (1993) and references thererin.

[6] B.D. Serot and J.D. Walecka, *Advances in Nuclear Physics*, Vol. **16** (Plenum, New York, 1986).

[7] M.V. Hynes, A. Picklesimer, P.C. Tandy and R.M. Thaler, Phys. Rev. **C31**, 1438 (1985).

[8] E.D. Cooper and B.K. Jennings, Nucl. Phys, **A458**, 717 (1986).

[9] M. Thies, Phys. Lett. **B162**, 255 (1985).

[10] J.W. Negele, Comments Nucl. Part. Phys. **14**, 303 (1985).

[11] T. Jaroszewicz and S.J. Brodsky, Phys. Rev. **C43**, 1946 (1991).

[12] E. Bleszynski, M. Bleszynski and T. Jaroszewicz, Phys. Rev. Lett. **59**, 423 (1987).

[13] S.J. Wallace, Franz Gross and J.A. Tjon, Phys. Rev. Lett. **74**, 228 (1995).

[14] L.S. Celenza, B. Goulard and C.M. Shakin, Phys. Rev. **D24**, 912 (1981).

[15] R. Brockmann and R. Machleidt, Phys. Rev. **C42**, 1965 (1990)

[16] Z.E. Meziani et al., Phys. Rev. Lett. **52**, 2130 (1984).

[17] J. Jourdan, Phys. Lett. **B353**, 189 (1995); Nucl. Phys, **A603**, 117 (1996).

[18] J. Morgenstern and Z.-E. Meziani, Phys. Lett. **B515**, 269 (2001); Eur. Phys. J. **A17** (2003) 451.

[19] M. Traini, Nucl. Phys. **A694**, 325 (2001).

[20] C.J. Horowitz, Phys. Lett. **B208**, 8 (1988).

[21] E.N. Nikolov, M. Bergmann, Chr.V. Christov, K. Goeke, A.N. Antonov and S. Krewald, Phys. Lett. **B281**, 208 (1992).

[22] J.V. Noble, Phys. Rev. Lett. **46**, 412 (1981).